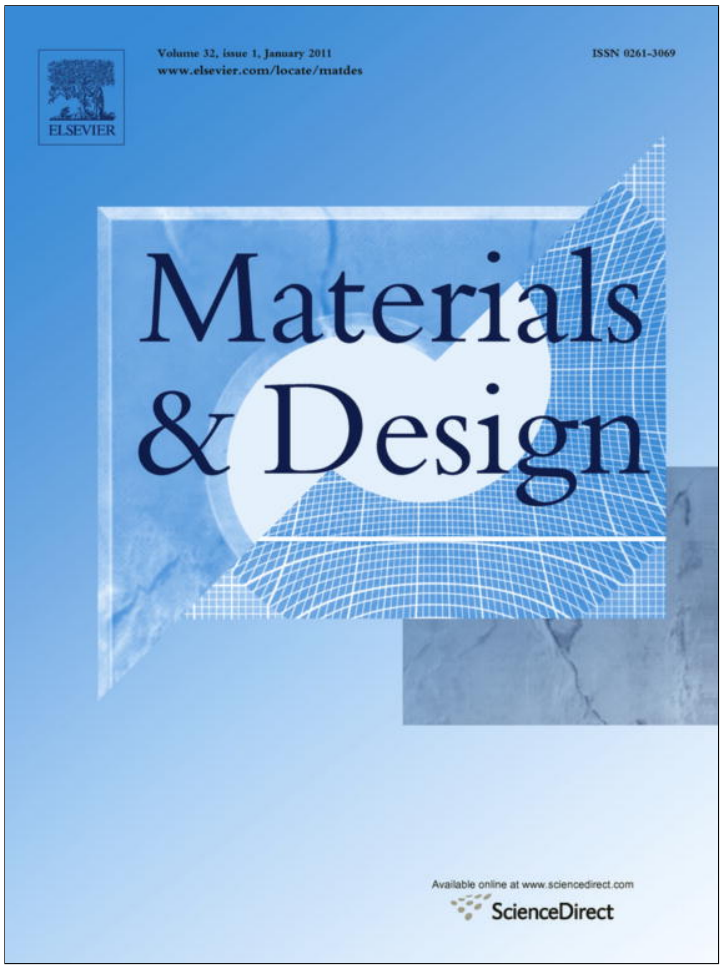
Provided for non-commercial research and education use.
Not for reproduction, distribution or commercial use.



(This is a sample cover image for this issue. The actual cover is not yet available at this time.)

This article appeared in a journal published by Elsevier. The attached copy is furnished to the author for internal non-commercial research and education use, including for instruction at the authors institution and sharing with colleagues.

Other uses, including reproduction and distribution, or selling or licensing copies, or posting to personal, institutional or third party websites are prohibited.

In most cases authors are permitted to post their version of the article (e.g. in Word or Tex form) to their personal website or institutional repository. Authors requiring further information regarding Elsevier's archiving and manuscript policies are encouraged to visit:

http://www.elsevier.com/copyright

Author's personal copy

Materials and Design 35 (2012) 113–119

Contents lists available at SciVerse ScienceDirect

Materials and Design

journal homepage: www.elsevier.com/locate/matdes

Technical Report

Application of Taguchi approach to optimize friction stir spot welding parameters of polypropylene

Mustafa Kemal Bilici *

Marmara University, Technical Education Faculty, Department of Materials Technology, Goztepe Campus, 34722 Istanbul, Turkey

ARTICLE INFO

Article history:
Received 22 July 2011
Accepted 22 August 2011
Available online 6 September 2011

ABSTRACT

This paper shows experimental and numerical results of friction stir spot welding of high density polypropylene. The determination of the welding parameters plays an important role for the weld strength. The experimental tests, conducted according to combinations of process factors such as tool rotation speed, plunge depth and dwell time at beginning welding, were carried out according the Taguchi orthogonal table L9 in randomized way. The Taguchi approach was used as a statistical design of experiment technique to set the optimal welding parameters. The results show coherence between the numerical predictions and experimental observations in different cases of weld strength. The signal-to-noise ratio and the analysis of variance were utilized to obtain the influence of the friction stir spot welding parameters on the weld strength. Finally, the improvement in the weld strength from the initial welding parameters to the optimal welding parameters was about 47.7%.

© 2011 Elsevier Ltd. All rights reserved.

1. Introduction

Modern thermoplastic materials are used in an expanding range of engineering applications, such as in the automotive industry, due to their enhanced stress-to-weight ratios, toughness, a very short time of solidification and a low thermal conductivity [1,2]. The critical trend in automotive manufacturing is the increasing use of lightweight alloys in place of traditional steel components. The use of aluminum alloys for auto body panels leads to a reduction in the vehicle body weight which translates into reduced emissions and increased performance. After the body panels are formed into the desired shapes they will require joining to other parts of the automobile [3].

Resistance spot welding is a very common joining technique in the automotive industry [4]. The resistance spot welding process (RSW) and can be used to replace on processes, such as riveting, RSW, screwing and any other punctual method. This welding process is widely used in the joining of sheet metal assemblies due to its advantages in welding efficiency and suitability for automation [5]. Global trends force the automotive industry to manufacture lighter, safer, more environmentally friendly and ultimately cheaper vehicles [6]. Reduction in vehicle weight can be obtained by replacing conventional steels and cast irons with advanced high strength steels and light weight materials, such as aluminum, magnesium and reinforced polymer composites [7–9]. Aluminum and other lightmetals joints have experienced problems in resistance spot welding. These problems are flush, wear, overheating and melting. Because of these problems, this method has been developed as an alternative method friction stir spot welding (FSSW). FSSW method is carried out easily combine with the light metals.

A new alternative welding technique has been recently developed by Mazda Motor Corporation and Kawasaki Heavy Industries, with over 90% in energy saving and 40% equipment saving [10]. Spot friction welding (also known as friction stir spot welding) offers an ability to join aluminum sheets at a much lower operating and investment cost compared to resistance spot welding. FSSW overcomes the inherent difficulties found in other methods, as high cost for fasteners, longer downtime caused by feeding issues and need for other operations [11,12].

In 2001, Friction stir spot welding (FSSW) was developed in the automotive industry to substitute resistance spot welding for aluminum sheets. FSSW process has some advantages such as ease of joining materials low distorsion, excellent mechanical properties, low cost and more economical than RSW [13]. The FSSW process consists of three phases; plunging, stirring and retracting as shown in Fig. 1 [13]. The process starts with spinning the tool with a high rotational speed. Then the tool is forced into the weld spot until the shoulder of the tool enters the surface of the upper workpiece. The plunge movement of the tool causes material to expel as shown in Fig. 1a and b. When the tool reaches the predetermined depth, the plunge motion ends and the stirring phase starts. In this phase, the tool rotates in the workpieces without plunging. Frictional heat is generated in the plunging and the stirring phase and, thus, the material adjacent to the tool is heated and softened. The softened upper and lower workpiece materials mix together in the stirring phase. The shoulder of the tool creates a compressional stress on the softened material. A solid-state joint is formed in the stirring

* Fax: +90 216 337 89 87.
E-mail address: mkbilici@marmara.edu.tr

0261-3069/$ - see front matter © 2011 Elsevier Ltd. All rights reserved.
doi:10.1016/j.matdes.2011.08.033

Author's personal copy

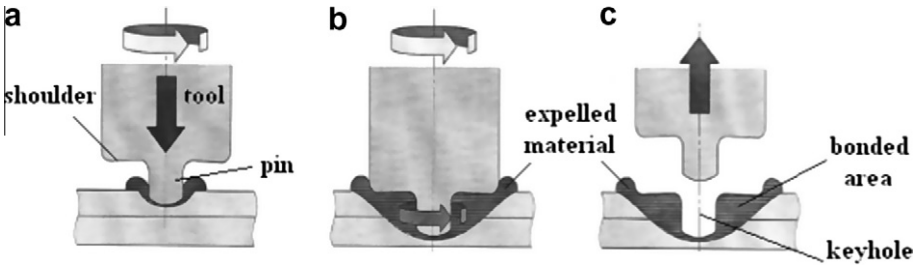


Fig. 1. Three phases of friction stir spot welding process, (a) plunging, (b) stirring and (c) retracting [14].

phase. When a predetermined bonding is obtained, the process stops and the tool is retracted from the workpieces. The resulting weld has a characteristic keyhole in the middle of the joint as shown in Fig. 1c. The tool geometry and welding parameters (tool rotational speed, tool plunge depth and dwell time) effect heat production, joint formation and strength of welds [14].

There are very few publications about polymer FSSW applications [15–17]. Arıcı investigated some friction stir spot welding parameters, therefore, this study was intended to explain the effects of all FSSW parameters on FSSW strength of polypropylene sheets. Basically, classical experimental design methods are too complex and not easy to use. A large number of experiments have to be carried out when the number of the welding parameters increases. To solve this problem, the Taguchi method uses a special design of orthogonal arrays to study the entire parameter space with only a small number of experiments [18–21]. The Taguchi design method has been found to be a simple and robust technique for optimizing the welding parameters [22].

The present study is performed to fulfil the following two objectives:

1. To use the Taguchi method for determining the efficiency ratio FSSW parameters.
2. To estimate the contribution of individual welding parameters to the strength of the weld joint.
3. Response table for weld strength were obtained.

2. Materials and methods

In this study, 4 mm thick polypropylene sheets were used. Fig. 2 shows a lap-shear specimen that was used to investigate the weld strength of the friction stir spot welds under shear loading conditions. The specimens were welded in a milling machine. In order to develop the FSSW tests, a properly designed clamping fixture was utilized to fix the specimens. Fig. 3 shows a properly designed clamping fixture. Fig. 4 illustrates a magnified cross sectional view of the tool used in the welding. The tool was machined from SAE 1050 steel and heat treated to a hardness of 40 HR_C. The lap-shear strength was obtained by averaging the strengths of five individual specimens, which were welded with identical welding parameters.

2.1. Experimental method

From the preliminary experimental results, three levels of welding parameters were selected as shown in Table 1. In this study an L_9 orthogonal array with four columns and nine rows was used [20]. The experimental layout for the three welding parameters using the L_9 orthogonal array is shown in Table 2. Since the L_9 orthogonal array has four columns, each welding parameter is assigned to a column, and the last column is left empty for the error in experiments [20]. The orthogonality is not lost by letting one column of the array remain empty.

The rotating tool plunged into the workpieces with a certain plunge rate to the required depth at an accuracy of ±0.02 mm. The stirring phase of FSSW started with the completion of the tool plunging. In this phase, the tool rotated without plunging. The duration of this phase is called the dwell time. Upon reaching the predetermined dwell time the rotation of the tool was immediately stopped. The tool stayed in the workpiece for 30 s and then it was retreated. All the welding operations were done at the room temperature. At the beginning of each welding operation, the pin and the shoulder of the tool were at room temperature.

Welded lap-shear specimens were tested on an Instron machine at a constant crosshead speed of 5 mm/s. The breaking force was recorded during the test. The lap shear strength was obtained by averaging the strengths of 5 individual specimens, which were welded with identical welding parameters.

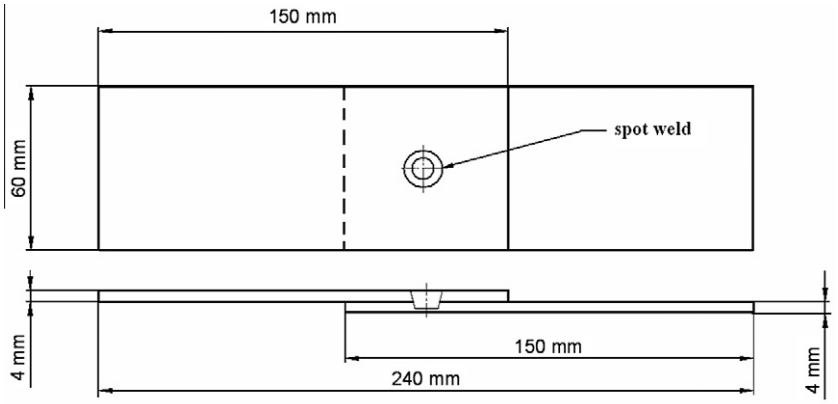


Fig. 2. Configuration of the lap-shear test specimen.

Author's personal copy

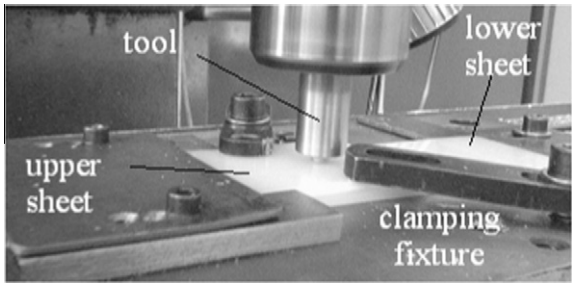


Fig. 3. A properly designed clamping fixture.

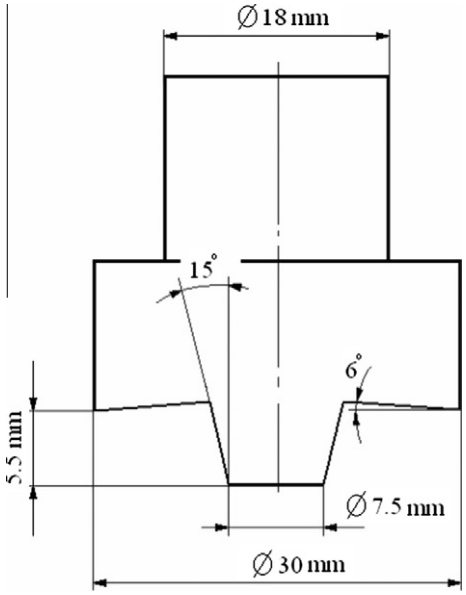


Fig. 4. A magnified cross sectional view of the tool.

Table 1
Welding parameters and their levels.

Symbol	Welding parameter	Unit	Level 1	Level 2	Level 3
A	Dwell time	s	50	100	150
B	Tool plunge depth	mm	5.7	6.2	6.7
C	Tool rotation speed	rpm	700	900	1100

Table 2
Experimental layout using an L_9 orthogonal array.

Experiment number	Welding Parameter			Error
	A Dwell time (s)	B Tool plunge depth (mm)	C Tool rotation speed (rpm)	D
1	50	5.7	700	
2	50	6.2	900	
3	50	6.7	1100	
4	100	5.7	1100	
5	100	6.2	700	
6	100	6.7	900	
7	150	5.7	900	
8	150	6.2	1100	
9	150	6.7	700	

2.2. Experimental design

The lap shear strength of designed experiments are shown in Table 3. The Taguchi method uses the signal to noise (S/N) ratio [19]. The last column of Table 3 shows the calculated S/N ratio of the experiments. The term 'signal' represents the desirable value (mean) for the output characteristic and the term 'noise' represents the undesirable value for the output characteristic. Therefore, the S/N ratio is the ratio of the mean to the square deviation (S.D). Taguchi uses S/N ratio to measure the quality characteristic deviating from the desired value. The S/N ratio (η) is defined as [20]:

$$\eta = -10\log(\mathrm{MSD}) \tag{1}$$

where MSD. is the mean square deviation for the output characteristic.

For the spot weld strength, the higher – the better quality characteristic is taken [22]. The MSD for the higher – the better quality is expressed as [20]:

$$\mathrm{MSD} = \frac{1}{n}\sum_{i=1}^{n}\frac{1}{T_i^2} \tag{2}$$

where n is the number of tests and T_i is the value of weld strength of the i th test. The Table 3 shows the experimental results for the weld strength and the corresponding S/N ratio which were calculated by using Eqs. (1) and (2).

In these tests, nine different welding parameter combinations were used. Therefore, The effect of each welding parameter on the weld strength cannot be clearly understood from the result of Table 3. A minitab statistical software was used to explain the welding parameter effect [23]. From the results of Table 3, diagrams were drawn to display the welding parameters effects on the weld strength.

3. Results

Fig. 5 shows the appearance of the test specimen after joining. As shown in the figure, the joining is completed without any deformation of the upper or lower sheet. As shown in Fig. 5, the shape of the tool is transferred onto the joint on the side into which the tool is pressed and the base metal that is pushed out by the tool forms a ring of excess metal around the weld. The effects of welding parameters (dwell time, tool rotational speed and tool plunge depth) on joint strength are shown in Figs. 6–8. These diagrams illustrate the combine effects of any two parameters on the weld strength. In each graph one welding parameter effect was omitted. The black zones of the diagrams show the weld strength over 3800 N. Only two parameters can be decided from a diagram. The effect of tool plunge depth is shown in Figs. 6 and 7. These two figure show that the tool plunge depth must be lower than 6.0 mm depth. Fig. 8 indicates that optimum joint strength can be obtained by using proper tool rotational speed and dwell time. The optimum rotational speed changes with the dwell time. If the dwell time is long a small rotational speed is needed. For example If the dwell time is 150 s the optimum rotational speed is 900 rpm. The optimum speed increases if the dwell time is short (Fig. 8). A definite optimum welding parameter combination cannot be determined from Figs. 6–8.

Since the experimental design is orthogonal, it is then possible to separate out the effect of each welding parameter at different levels. For example, the mean S/N ratio for tool rotation speed at levels 1, 2 and 3 can be calculated by averaging S/N ratios for the experiments 1–3, 4–6, and 7–9, respectively [13]. These results are illustrated in the first row of Table 4. Table 4 shows the mean S/N ratio for each level of the welding parameters. This table is named as the S/N response table for the weld strength. The total

Author's personal copy

Table 3
Experimental results for weld strength and calculated S/N ratios.

Experiment number	Lap-shear fracture force (N)	Calculated S/N ratio (dB)
1	1892	65.54
2	2327	67.34
3	1826	65.23
4	3984	72.01
5	3525	70.94
6	3070	69.74
7	4126	72.31
8	2884	69.20
9	2453	67.7 9

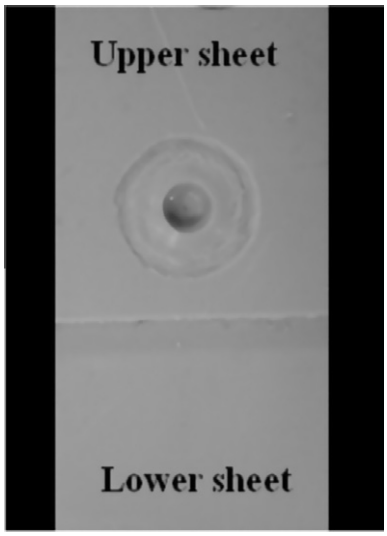


Fig. 5. Appearance of a friction stir spot weld joint.

mean S/N ratio (η_m) of the nine experiments was calculated as 68.90 dB.

The S/N response graph (Fig. 9) for weld strength was drawn with using the results given in Table 4. In Fig. 9 the dashed line shows the total mean S/N ratio (68.90 dB) of the experiments. The graphs of Fig. 9 show the level effects of each welding parameter. For example, the mean S/N ratio decreases from B1 to B3. That means that the weld strength decreases with the increase of the plunge depth. The effect of the dwell time is similar to the effect the tool rotational speed. The S/N ratio is very is low at A1. The maximum S/N ratio is obtained at A2. The S/N ratio decreases with increasing the dwell time from A2 to A3. The tool rotational speed shows the same trend. In this study, the dwell time has been determined to be the most effective parameter on S/N ratio.

3.1. Analysis of variance

The relative importance among the welding parameters on weld strength is needed to be determined so that optimal combinations of the parameter levels can be assessed accurately. This can be achieved by using the analysis of variance. The purpose of the analysis of variance (ANOVA) is to investigate the importance of the welding parameters on the quality characteristic [13]. This is accomplished by separating the total variability of the S/N ratios, which is measured by the sum of the squared deviations from the total mean S/N ratio, into contributions by each of the welding parameters and the error. First, the total sum of squared deviations (SS_T) from the total mean S/N ratio (η_m) can be calculated as [18].

$$SS_T = \sum_{i=1}^{n} (\eta_i - \eta_m)^2 \quad (3)$$

where n is the number of experiments in the orthogonal array and n_i is the mean S/N ratio for the i th experiment. In this study n was equal to nine. The total sum of spared deviations SS_T is decomposed into two sources: the sum of squared deviations (SS_d) due to each design parameter and the sum of squared error (SS_e). The percentage contribution ρ by each of the design parameters in the total sum of squared deviations (SS_d) is a ratio of the sum of squared deviations (SS_e) due to each design parameter to the total sum of squared deviations (SS_T) [19]. Statistically, there is a tool called an F test named after Fisher to see which design parameters have a significant effect on the quality characteristic. In performing the F test, the mean of squared deviations (SS_m) due to each design parameter needs to be calculated. The mean of squared deviations (SS_m) is equal to the sum of squared deviations (SS_d) divided by the number of degrees of freedom associated with the design parameter. Then, the F value for each design parameter is simply the ratio of the mean of squared deviations (SS_m) to the mean of squared error. Usually, when $F > 4$, it means that the change of the design parameter has a significant effect on the quality characteristic [24].

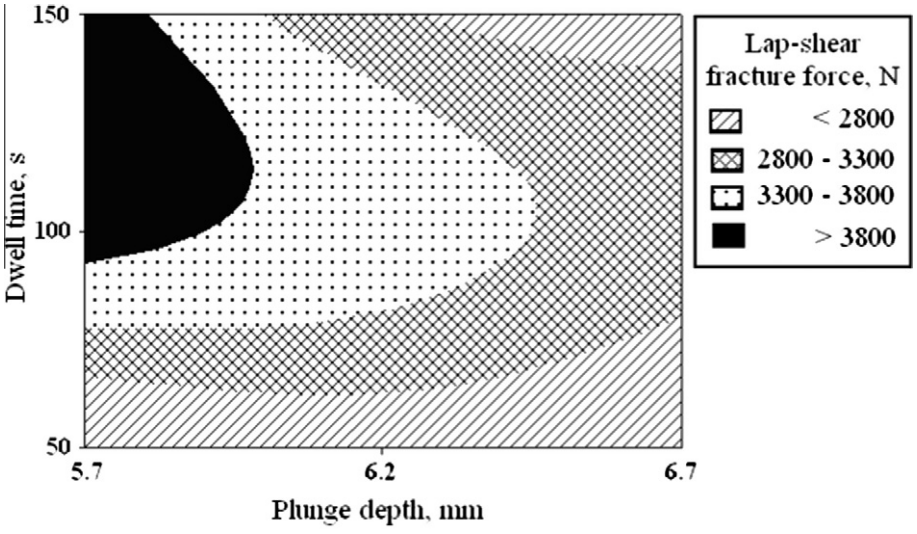


Fig. 6. ANOVA analyses, the optimal welding parameters (dwell time and plunge depth) for weld strength.

Author's personal copy

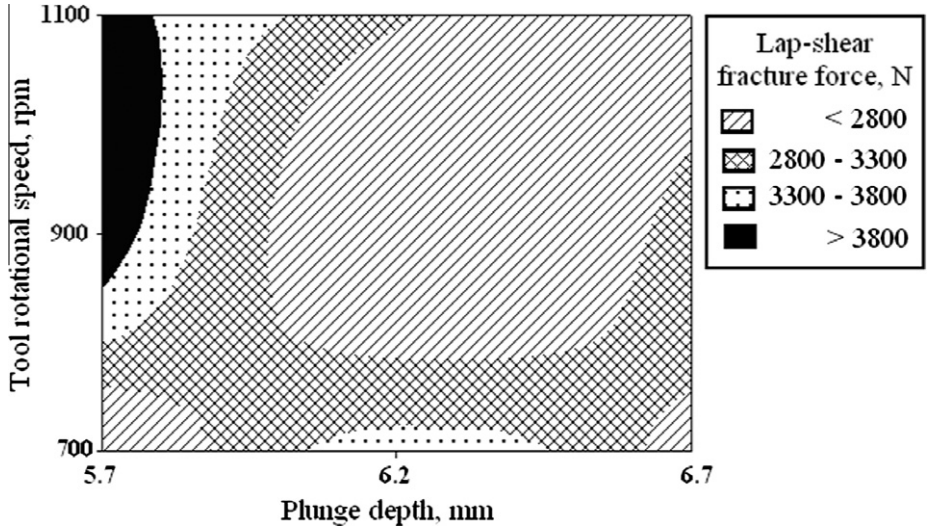


Fig. 7. ANOVA analyses, the optimal welding parameters (tool rotational speed and plunge depth) for weld strength.

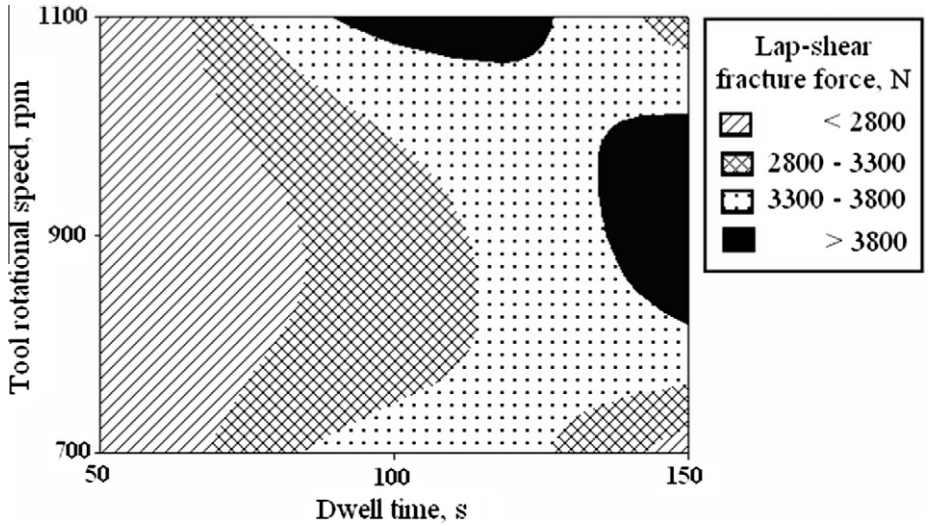


Fig. 8. ANOVA analyses, the optimal welding parameters (tool rotational speed and dwell time) for weld strength.

Table 4
S/N response table for weld strength.

Symbol	Welding parameter	Mean S/N ration (dB)				
		Level 1	Level 2	Level 3	Max–min	Rank
A	Dwell time	66.03	70.90	69.77	4.87	1
B	Tool plunge depth	69.95	69.16	67.59	2.36	2
C	Tool rotation speed	68.09	69.80	68.81	1.71	3

The total mean S/N ratio = 68.90 dB.

4. Discussion

Table 5 shows the results of ANOVA on weld strength. The *F* value of a welding parameter shows the effectiveness of the parameter. The welding parameter which has the highest degree is the most important parameter [20]. The *F* value of the dwell time is the highest (14.88). It is found that dwell time is very important in polypropylene FSSW, because it has the greatest *F* value the tool plunge depth is found to be second important welding parameter. The tool rotation speed was found to be the least effective factor on the weld strength, because it has the lowest *F* quantity (1.69). The effects of welding parameters on weld strength are shown in Figs. 6–8. From these figures the optimal welding parameters for weld strength over 3800 N cannot be predicted precisely. From these figures only the optimum tool plunge depth was determined. Optimal welding parameters can be determined by using the graphs of Fig. 9.

Once the optimal level of the design parameters has been determined, the final step is to predict and verify the improvement of the quality characteristic using the optimal level of the design parameters [18]. The estimated S/N ratio ($\hat{\eta}$) using the optimal level of the design parameters can be calculated as:

$$\hat{\eta} = \eta_m + \sum_{i=0}^{o} (\bar{\eta}_i - \eta_m) \tag{4}$$

where (η_m) is the total mean S/N ratio, ($\bar{\eta}_i$) is the mean S/N ratio at the optimal level, and *o* is the number of the main design parameters that affect the quality characteristic.

The predicted S/N ratio using the optimal welding parameters for weld strength is determined as A2B1C2 from S/N and ANOVA

Author's personal copy

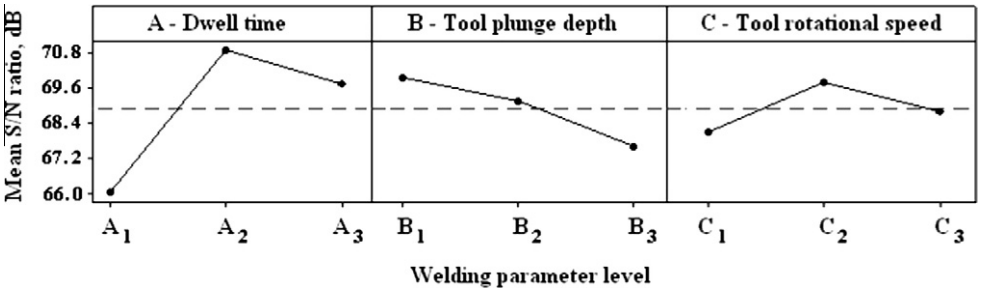


Fig. 9. The mean S/N response graph for weld strength.

Table 5
Results of the analysis of variance (ANOVA) for weld strength.

Symbol	Welding parameters	Degrees freedom	Sum of squares	Mean square	*F* ratio	Contribution (%)
A	Dwell time	2	38.9814	19.4907	14.88	71.3
B	Tool plunge depth	2	8.6586	4.3293	3.31	15.8
C	Tool rotation speed	2	4.4226	2.2113	1.69	8.1
Error		2	2.6190	1.3095		4.8
Total		8	54.6816			100.0

Table 6
Results of the confirmation experiment.

	Initial welding (Experiment)	Optimal welding parameters		Improvement
		Prediction	Experiment	
Parameter levels	A3B2C3	A2B1C2	A2B1C2	
Fracture force (N)	2884	4390	4260	1376
Calculated S/N ratio (dB)	69.20	72.85	72.59	3.39

analysis. Five welds were done with A2B1C2 welding parameters and their average weld strength was obtained. Table 6 shows the comparison of the predicted weld strength and actual weld strength of this weld. The S/N ratio of the test was calculated by using Eqs. (1) and (2). There is a good agreement between the predicted and actual weld strength values. The initial parameters were chosen as A3B2C3 from Fig. 9. With these initial welding parameters average weld strength was obtained (Table 3. experiment 8). The experimental strength result and the calculated S/N ratio of the weld using A3B2C3 parameters are shown on the first column of Table 6. The confirmation experiments show that the S/N ratio is improved by 3.39 dB and the weld strength is increased 1376 N from the initial welding parameters to the optimal welding parameters (Table 6.). The weld strength gain is about 47.7%. The large number of parameters affecting the mechanical properties of welded joints requires planning characterization tests; this reduces time and cost of experiments. The obtained results showed the feasibility of welding operations as well as good mechanical properties of polypropylene mechanical assemblies; they could be comparable to the base material. This is a future subject of investigation where the modeling, identification and numerical simulation take all their dimensions to predict the polymer welded structures behavior.

The experiments recorded during different welding show that in the range of rotation speed 700–1100 rpm, plunge depth 5.7 and 6.7 mm and dwell time 50 and 150 s, the reached weld strength levels vary between 2800 and 3800 N. This proves that the welding of polypropylene is produced in a liquid state by melting the material. Indeed, the polypropylene thermal properties are favorable to reduction in the heat affected zone size. The comparison between experimental observations and numerical predictions for the tensile tests of welded samples indicates that mechanical properties of weld joints are dependent on welding parameters. For safe welded parts, two behaviors were observed. The first corresponds to the presence of a weld joints more deformable than the base material; the second corresponds to the presence of mechanical scission. This finding lets admitting to the existence of an intermediate configuration of operational parameters for obtaining weld joint with mechanical properties very close to the base material. The welding parameters (dwell time, the tool plunge depth and the tool rotation speed) were observed very effective and important on weld strength of polypropylene friction stir spot welding.

5. Conclusions

The effect of friction stir spot welding parameters of polypropylene sheet weld strength was evaluated with the help of the Taguchi method. The following results were obtained by the experimental and the analytic results:

- The result of ANOVA proved that the quadratic mathematical models allow prediction of weld parameter with a 95.2% confident interval.
- The large number of parameters affecting the mechanical properties of welded joints requires planning characterization tests; this reduces time and cost of experiments.
- The dwell time, the tool plunge depth and the tool rotational speed were effective on joint strength of polypropylene FSSW.
- The dwell time was the most dominant welding parameter and the tool rotational speed was the least important welding parameter.
- The optimum welding parameters for the weld strength are roughly the dwell time of 100 s, the tool plunge depth of 5.7 mm and the tool rotation speed of 900 rpm.
- The improvement in the weld strength from the initial welding parameters to the optimal welding parameters was about 47.7%.

Acknowledgements

This work was supported by Scientific Research Project Program of Marmara University (Project No. FEN-C-DRP–010710–230). The authors are grateful to Marmara University for their financial

Author's personal copy

support and the provision of laboratory facilities. The author gratefully acknowledges adviser Ahmet Irfan YUKLER for his contributions to this work.

References

[1] Awang M, Mucino VH, Feng Z, David SA. Thermo-mechanical modeling of friction stir spot welding (FSSW) process: use of an explicit adaptive meshing scheme. SAE Int 2006;01:1392.
[2] Feng AH, Xiao BL, Ma ZY. Grain boundary misorientation and texture development in friction stir welded SiCp/Al–Cu–Mg composite. Mater Sci Eng A 2008;497:515–8.
[3] Yang CW, Hung FY, Lui TS, Chen LH, Juo JY. Weibull Statistics for evaluating failure behaviors and joining reliability of friction stir spot welded 5052 aluminum alloy. Mater Trans 2009;50(01):145–51.
[4] Aslanlar S, Ogur A, Ozsarac U, Ilhan E. Welding time effect on mechanical properties of automotive sheets in electrical resistance spot welding. Mater Des 2008;29:1427–31.
[5] Goodarzi M, Marashi SPH, Pouranvari M. Dependence of overload performance on weld attributes for resistance spot welded galvanized low carbon steel. J Mater Process Technol 2009;209:4379–84.
[6] Blawert C, Hort N, Kainer KV. Automotive applications of magnesium and its alloys. Trans Indian Inst Met 2004;57:397–408.
[7] Davies G. Future trends in automotive body materials. Mater Automob Bodies 2003;8:252–69.
[8] Cole GS, Sherman AM. Light weight materials for automotive applications. Mater Charact 1995;35:3–9.
[9] Matsuyama K. Trend of automobile vehicles and the joining technologies. Inter Weld Ins Documents IIW- Doc III 2006;06:1386.
[10] Lathabai S, Painter MJ, Cantin GMD, Tyagi VK. Friction stir spot welding of automotive lightweight alloys. Proceedings of the 7th international conference on trends in welding research May 16–20; 2005. Georgia USA.
[11] Hancock R. Friction welding of aluminium cuts energy cost by 99%. Weld J 2004;83:40.
[12] Wanga DA, Leeb SC. Microstructures and Failure Mechanisms of Friction Stir Spot Welds of Aluminum 6061-T6 Sheets. J Mater Proc Technol 2007;186:291–7.
[13] Lin TR. Experimental design and performance analysis of TiN coated carbide tool in face milling stainless steel. J Mater Proc Technol 2002;127:1–7.
[14] Buffa G, Fratini L, Piacentini M. On the influence of tool path in friction stir spot welding of aluminium alloys. J Mater Process Technol 2008:208–317.
[15] Oliveria PHF, Filho STA, Santos JF, Hage E. Preliminary study on the feasibility of friction spot welding in PMMA. Mater Lett 2010;64:2098–101.
[16] Arıcı A, Mert S. Friction stir spot welding of polypropylene. J Reinf Plast Compos 2008;27:2001–4.
[17] Bilici MK, Yukler AI, Kurtulmuş M. The optimization of welding parameters for friction stir spot welding of high density polyethylene sheets. Mater Des 2011;32:4074–9.
[18] Mazundar SK, Hoa SV. Application of Taguchi method for process enhancement of on-line consolidation technique. Composites 1995;26:669–763.
[19] Ross PJ. Taguchi techniques for quality engineering. New York: Mc-Graw Hill; 1988.
[20] Peace GS. Taguchi methods. New York: Addison-Wesley; 1993.
[21] Tarng YS, Juang SC, Chang CH. The use of grey based Taguchi methods to determine submerged arc welding process parameters in hardfacing. J Mater Process Technol 2002;128:1–6.
[22] Juang SC, Tarng YS. Process parameter selection for optimizing the weld pool geometry in the tungsten inert gas welding of stainless steel. J Mater Process Technol 2002;122:33–7.
[23] Minitab User Manual (Release 15). Making data analysis easier. MINITAB Inc. State College, PA: USA; 2001.
[24] Yang WH, Tarng YS. Design optimization of cutting parameters for turning operations base on the Taguchi method. J Mater Process Technol 1998;84:122–9.